Journal of Applied Electrochemistry (2006) 36:1143–1149
DOI 10.1007/s10800-006-9197-9

Electrocatalytic behaviour for oxygen reduction reaction of small nanostructured crystalline bimetallic Pt–M supported catalysts

A. STASSI[1], C. D'URSO[1], V. BAGLIO[1], A. DI BLASI[1], V. ANTONUCCI[1], A.S. ARICO[1,*], A.M. CASTRO LUNA[2], A. BONESI[2] and W.E. TRIACA[2]
[1]*CNR-ITAE, Via Salita S. Lucia sopra Contesse 5, 98126, Messina, Italy*
[2]*INIFTA, Universidad National de La Plata, Sucursal 4, CC 16, 1900, La Plata, Argentina*
*(*author for correspondence, fax: + 39-090-624247, e-mail: arico@itae.cnr.it)*

Received 16 January 2006; accepted in revised form 27 June 2006

Key words: DMFC, methanol tolerance, oxygen reduction reaction, Pt–Cu catalyst, Pt–Fe catalyst

Abstract

A 60 wt% Pt–Fe/C and a 60 wt% Pt–Cu/C catalysts with Fe and Cu content of 5 wt% were prepared by using a combination of colloidal and incipient wetness methods; this has allowed synthesis of small nanostructured crystalline bimetallic catalysts with particle size less than 3 nm and with a suitable degree of alloying. These materials were studied in terms of structure, morphology and composition using XRD, XRF and TEM techniques. The electrocatalytic behaviour for ORR of the catalysts was investigated using the rotating disk technique and compared to that of a pure Pt catalyst with similar particle size. No improvement in performance was recorded with the Pt–Cu compared to Pt catalyst, whereas, a promoting effect in enhancing the ORR was observed for the Pt–Fe catalyst both with and without methanol in the oxygen-saturated electrolyte solution.

1. Introduction

The direct methanol fuel cell (DMFC) is an attractive device as a power source for applications in transportation and in portable electronic systems because of its high energy density and because it can operate at ambient conditions [1–4]. DMFC uses a potentially renewable fuel source, easy to store and transport. Even though good progress has been made in the development of DMFC anode catalysts, there are still some problems that need to be addressed, one of which is related to the cross-over of methanol from the anode to the cathode through the proton exchange membranes. Methanol crossover results in a significant loss in efficiency of a DMFC because on the Pt cathode two reactions compete, i.e. O_2 reduction (ORR) and CH_3OH oxidation. One possibility to solve this problem is to use an oxygen reduction catalyst, inactive towards methanol oxidation or having a high methanol tolerance [5]. Thus, it is necessary to develop novel Pt based electrocatalysts that can catalyze the oxygen reduction but limit methanol oxidation. Many investigations have shown that some binary Pt based alloy catalysts, such as Pt–M, (where M = Co, Fe, etc.), exhibit an enhanced electrocatalytic activity for the ORR in comparison with Pt alone [6–11]. Such an activity enhancement was explained by the increased Pt d-band vacancy (electronic factor) and by the favorable Pt–Pt interatomic distance (geometric effect).

A relationship between the electrocatalytic activity and the adsorbate bond length has been predicted. Thus, a lattice contraction due to alloying would result in a more favorable Pt–Pt distance for the dissociative adsorption of O_2. Besides this, an interplay between electronic and geometric factors (Pt d-band vacancy and Pt-coordination numbers) and its relative effect on the OH chemisorption from the electrolyte occurs [12].

Watanabe et al. reported that, after electrochemical testing of a Pt–Fe alloy, the catalyst was covered by a thin Pt skin of less 1 nm thickness [13]. Moreover, they suggested that during the adsorption step, a π orbital of O_2 interacts with empty d orbitals of Pt and consequent back donation from the partially filled orbital of Pt to π^* (anti-bonding) molecular orbital of O_2. The increase in d band vacancies on Pt by alloying produces a strong metal–O_2 interaction. This interaction weakens the O–O bonds, resulting in bond cleavage and bond, formation between O and H^+ of the electrolyte, thus improving the ORR. One concern with Pt alloys in fuel cells is dissolution of transition metal. Pourbaix diagrams [14] indicate that most metals such as Co, Cu, Fe, Ni, etc. are soluble at a potential between 0.3 and 1 V versus SHE and at low pH values. The dissolution of the transition metal would cause an increase in surface area of the residual Pt catalyst.

There are different procedures related to catalyst preparation for DMFCs [15, 16]. Preparation methods such as impregnation, colloidal deposition and surface reduction involve the adsorption of active compounds on a carbon black surface [17]. The synthesis of a highly dispersed electrocatalyst phase in conjunction with high metal loading on a carbon support is one of the present goals in DMFCs. Most of the previous studies were dealing with catalysts characterized by particle size larger than about 4 nm and low concentration of active phase on carbon due to the need of high temperature treatment to form bimetallic alloys of transition metals with Pt [6–11]. However, in order to accelerate the oxygen reduction process a suitable number of surface sites is necessary. Furthermore, various studies have indicated that for supported Pt/C catalysts a maximum catalytic activity occurs at about 3 nm as a suitable compromise between number of sites and crystallographic phases with low Miller index characterized by high intrinsic activity [18].

The aim of the present work is to study the electrochemical behaviour of different supported high metal loading binary Pt based catalysts for the oxygen reduction in the presence of methanol with transition metals, such as Fe and Cu. A colloidal preparation procedure developed at ITAE Institute has allowed synthesis of alloyed bimetallic catalysts with particle size less than 3 nm [19]. The oxygen reduction reaction properties, together with methanol tolerance characteristics, of these bimetallic catalysts are examined and interpreted in the light of the structure, chemical and surface properties. The goal is to provide a contribution to the understanding of the catalytic properties for ORR of small nanostructured crystalline bimetallic Pt–M supported catalysts highly concentrated on the surface of a carbon black support.

2. Experimental

Platinized carbon was prepared by using the sulfite-complex route [17, 19]. A $Na_6Pt(SO_3)_4$ precursor was obtained from chloroplatinic acid. A Vulcan XC-72R carbon black was suspended in distilled water and agitated in an ultrasonic water bath at about 80 °C to form a slurry. The appropriate amount of $Na_6Pt(SO_3)_4$ was successively added to the slurry. The Pt sulfite complex solution was decomposed by adding H_2O_2, to form colloidal PtO_x/C. Subsequently, 60% Pt/C was obtained by reducing the PtO_x/C in a H_2/He stream.

The Pt/C catalyst was characterized by recording the powder X-ray diffraction (XRD) pattern on a Philips X-pert 3710 X-ray diffractometer using CuKα radiation operating at 40 eV and 30 mA. The peak profile of the (220) reflection in the face centered cubic structure was obtained by using the Marquardt algorithm. The Pt/C showed a particle size of 2.8 nm. A 60 wt% Pt–Fe/C and a 60 wt% Pt–Cu/C with a 5 wt% of transition metals (Fe, Cu) and a catalyst atomic composition of about Pt_3M_1 were prepared starting from PtO_x/C. To prepare the 60 wt% Pt–Fe/C and Pt–Cu/C catalysts, an impregnation procedure was employed. The bimetallic catalysts were reduced in a H_2 stream at room temperature. X-ray Fluorescence analysis of the catalysts was carried out by a Bruker AXS S4 Explorer spectrometer operating at a power of 1 kW and equipped with a Rh X-ray source, a LiF 220 crystal analyzer and a 0.12° divergence collimator. The Pt/M atomic ratio was determined in all catalyst samples. Table 1 shows the physico-chemical characteristics of the carbon supported Pt and Pt–M catalysts.

Table 1. Physico-chemical characteristics of Pt and Pt–M/C catalysts

Catalysts	Particle size /nm	A_0/nm	Pt/M at. (XRF)
60% Pt/C	2.8	0.392	–
60% Pt–Fe/C	2.4	0.390	3.33
60% Pt–Cu/C	2.1	0.387	3.79

To examine the ORR activity of the catalysts, the rotating disk technique was employed. Thus, the catalysts were electrochemically characterized employing a thermostated standard three-electrode cell, the rotating disk electrode consisted of glassy carbon rod (0.125 cm^2 geometric area) covered by a thin layer of catalyst embedded in a Nafion polymer electrolyte film [20]. A Pt foil was used as counter electrode and a saturated calomel electrode as reference electrode, the latter separated from the working electrode section by a closed electrolyte bridge to avoid chloride contamination. The potentials in this work are referred to that of the reversible hydrogen electrode (RHE). The electrolyte solution was 0.5 M H_2SO_4. The electrochemical experiments were conducted at different temperatures from 25 to 60 °C. Before working on ORR experiments, the disk composite electrode was cycled for 5 min at 0.1 V s^{-1} between 0.05 and 1.2 V in a N_2 purged sulfuric electrolyte solution to clean the surface. Subsequently, O_2 was bubbled in the solution and after 40 min, hydrodynamic current potential experiments were recorded by sweeping the potential from 1.0 to 0.2 V at 5 mV s^{-1} under rotating rate between 200 and 1500 rpm.

3. Results and discussion

The strategy adopted with the cathode catalysts was to synthesize formulations containing a high concentration of active catalytic phase on carbon whilst maintaining an appropriate particle size. The first approach concerned with the preparation of a 60% Pt/C catalyst with particle size around 3 nm. The structure and morphology of the prepared catalyst is shown in Figures 1 and 2. The XRD pattern of the Pt/C catalyst shows the typical fcc crystallographic structure (Figure 1). TEM analysis of the catalyst shows good dispersion of the Pt particles on the carbon support (Figure 2).

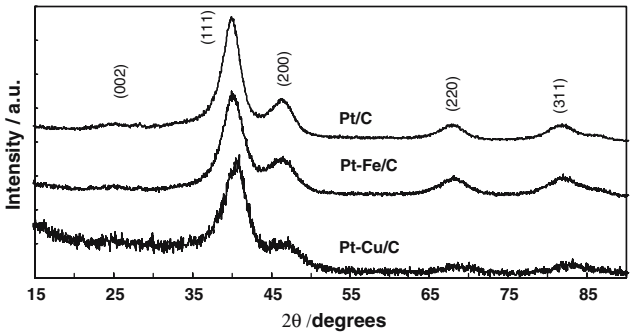

Fig. 1. XRD patterns of 60% Pt/C and 60% Pt–5% M/C catalysts. 002 reflection indicates the carbon black.

The second approach concerned with the preparation of 60% Pt–5% M/C catalysts with M = Fe, Cu. The aim was to modify the Pt surface by transition metals, using a low temperature preparation route which does not significantly increase the particle size as in conventional Pt–M catalysts treated at 700–900 °C. The data reported in Table 1 show a moderate degree of alloying of Fe with Pt as indicated by the slight decrease of the lattice parameter; whereas, a significant lattice contraction was found for the Pt–Cu catalysts. The particle size remains quite small, in the range between 2.1 and 2.4 nm, and the structure-morphology investigations show a single fcc phase and a homogeneous distribution of fine metal particles on the support (Figures 1 and 2). The particle size distribution histograms for all catalysts are reported in Figure 3. An unimodal particle size distribution is observed with particle sizes ranging from 1 to 5 nm.

Polarization curves for ORR for different catalysts, namely Pt, Pt–Cu and Pt–Fe, in an oxygen saturated sulfuric solution at 60 °C and 1000 rpm are shown in Figure 4. Similar electrocatalytic behaviour was observed for Pt and Pt–Cu catalysts; whereas the onset potential for the ORR on Pt–Fe catalyst is shifted towards higher potential, indicating better catalytic characteristics of this alloy for ORR compared to the previous ones. Thus, due to the better performance, our attention was focused on Pt–Fe rather than on Pt–Cu. The influence of temperature change on the Pt–Fe performance is reported in Figure 5. An enhancement both activation and mass transport properties is observed as the temperature is increased. Similar enhancement has been observed for Pt–Cu and Pt catalysts (not shown) indicating a similar activation mechanism. The electrochemical behaviour of Pt–Fe was also investigated in the presence of methanol in the acidic solution (Figure 6) and compared to the Pt catalyst. Figure 7 shows the current density-potential profile for the ORR reaction on Pt and Pt–Fe catalysts with and without methanol in the solution at 1000 rpm. Both catalysts showed a decrease in performance in the presence of methanol; this effect is more noticeable with increasing methanol concentration (Figure 6) or lowering of the rotation rate (not shown). With a methanol concentration of 0.05 M, a shift towards lower potentials

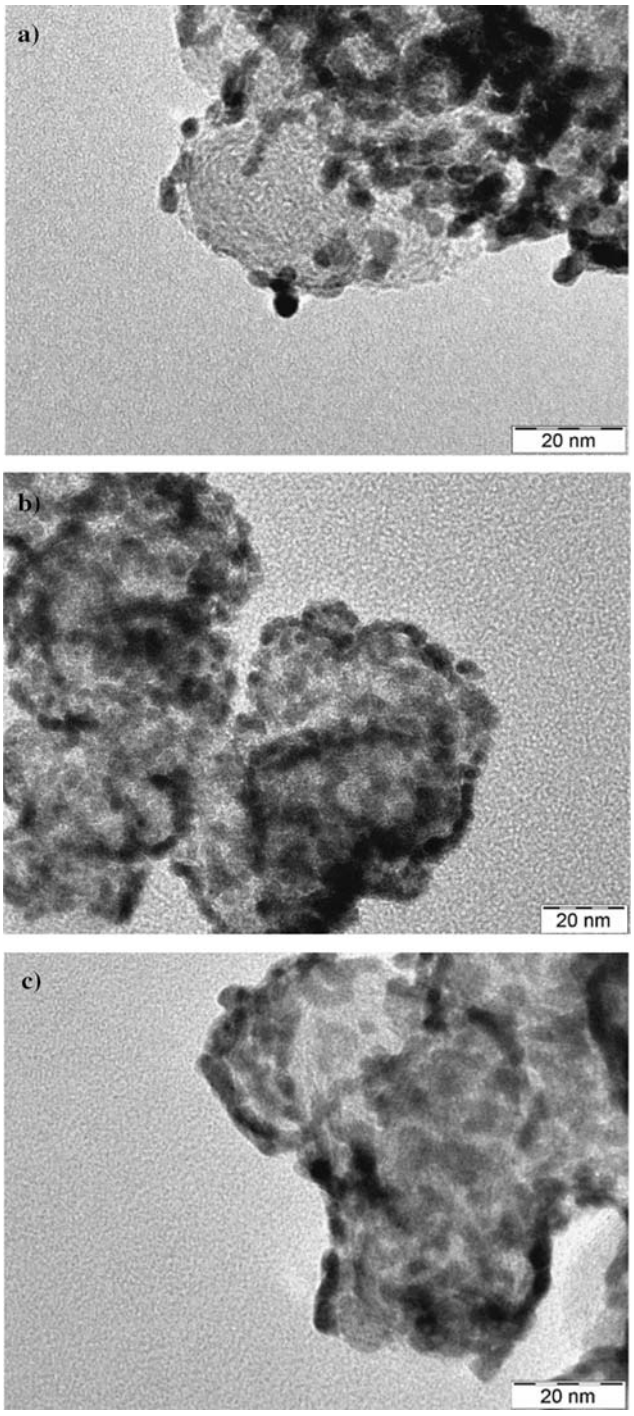

Fig. 2. TEM micrographs of (a) 60% Pt, (b) 60% Pt–Fe/C and (c) 60% Pt–Cu/C catalysts.

was observed for both catalysts. However, the polarization curve on the Pt–Fe catalyst is less negatively shifted in the presence of methanol than that on Pt; this clearly indicates a promoting effect of the bimetallic catalyst in enhancing the ORR and a better tolerance to methanol. At potentials lower than 0.7 V, the performance of the Pt–Fe catalyst in the presence of methanol appears to be similar to that of Pt without alcohol. Similar methanol tolerance properties were found for Pt–Ni catalysts by Lamy and coworkers [21]; these were ascribed to a

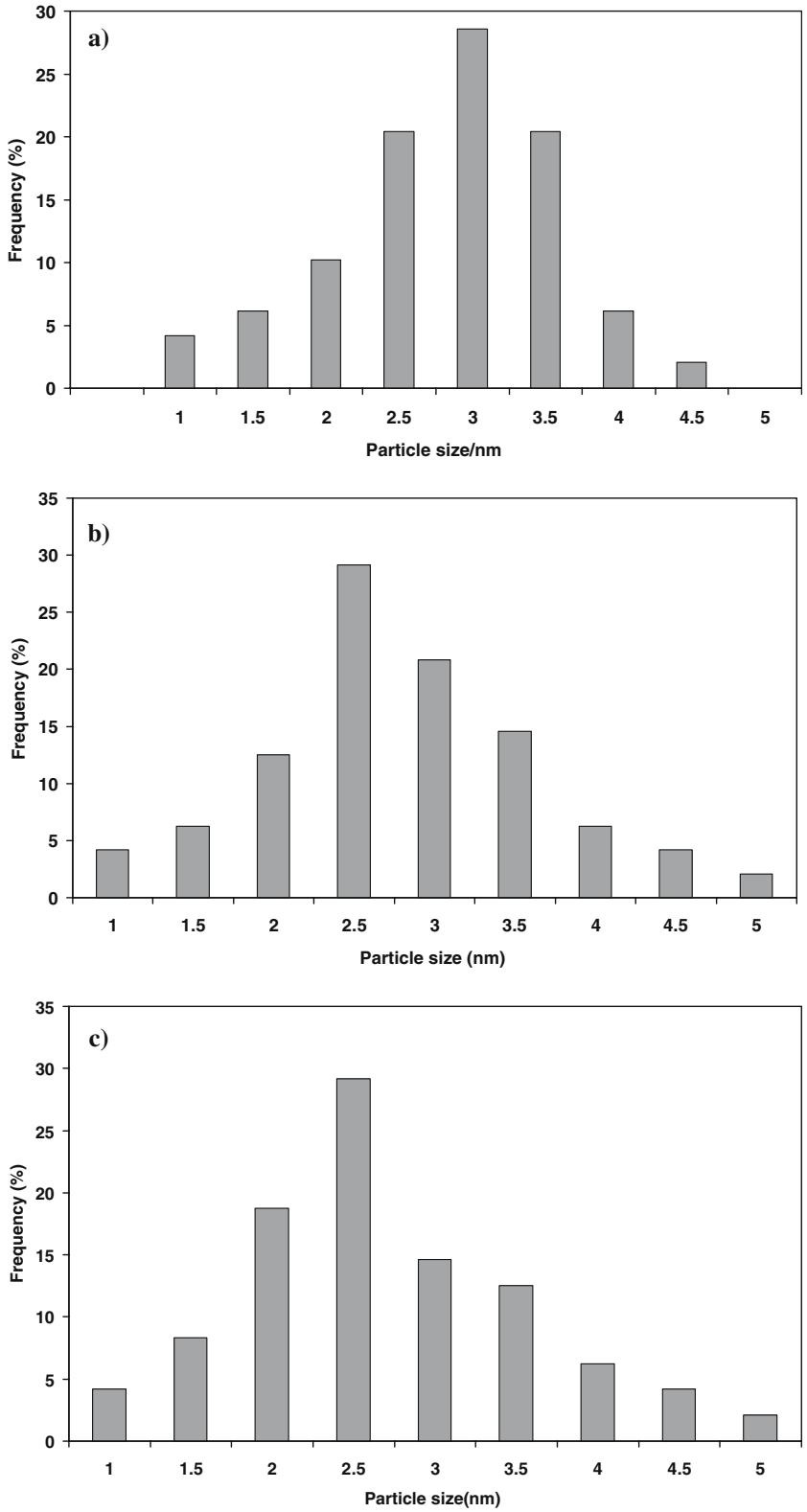

Fig. 3. Histograms of particle size distribution for (a) 60% Pt, (b) 60% Pt–Fe/C and (c) 60% Pt–Cu/C catalysts.

lowered activity for methanol oxidation. In order to get more insights on the mechanism, a Tafel analysis was carried out (see below).

Polarization curves for ORR on Pt–Fe electrode were measured at different rotation speeds (Figure 8). The limiting current densities increase progressively as the rotation speed was increased, as expected. The curves obtained at 1000 rpm were selected to determine the electro-kinetic parameters.

Tafel plots for the oxygen reduction process were obtained after correction for the oxygen mass transport effects; the contribution of the film diffusion resistance

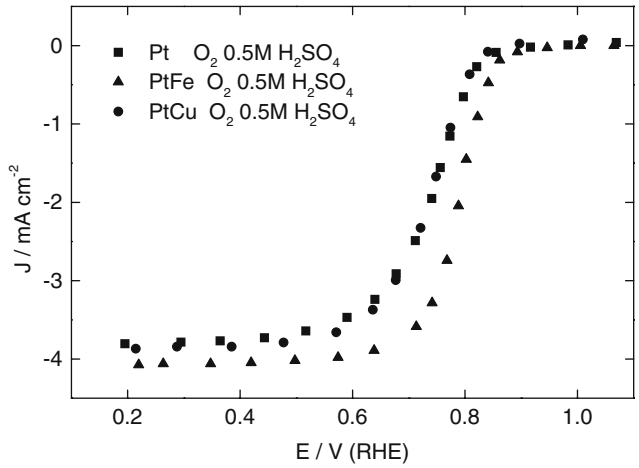

Fig. 4 Polarization curves for ORR in 0.5 M H_2SO_4, 60 °C, on Pt/C, Pt–Cu/C and Pt–Fe/C cathode catalysts.

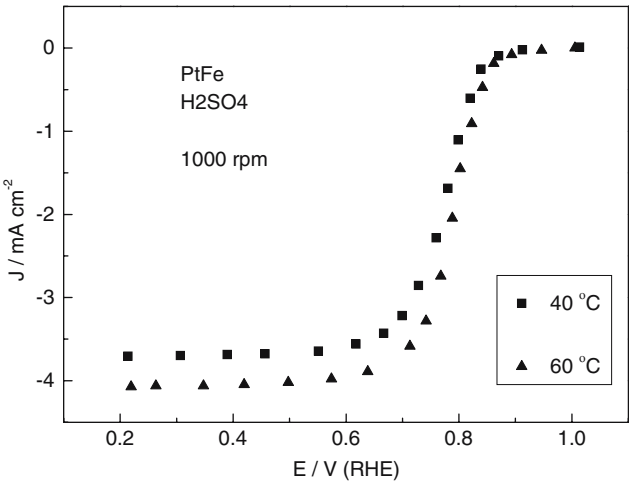

Fig. 5. Polarization curves for ORR in 0.5 M H_2SO_4 at 40 °C and 60 °C, on Pt–Fe/C cathode catalyst.

to the measured current density is considered negligible [20]. At any cathode potential E, the current density J was calculated as $(J \times J_l)/(J_l - J)$, where J and J_l are the measured and the limiting current density, respectively. Assuming that the polarization behaviour after mass transport correction is mainly activation controlled, the corresponding Tafel plots (Figure 9) in the range $0.6 < E < 0.9$ V were determined. Within the fitting error, the Tafel slope obtained at high potentials, ($E > 0.75$ V) on both Pt and Pt–Fe, was *ca.* 0.065 V decade^{-1}; and at low potentials ($E < 0.75$ V) *ca.* 0.120 V decade^{-1}. It seems that there is no dependence of ORR mechanism on the composition and structural parameters of the catalysts. The exchange current densities for the Pt and Pt–Fe catalysts, determined in the region characterized by 0.120 V decade^{-1} Tafel slope, were 1.63 10^{-5} mA cm^{-2} and 2.15 10^{-4} mA cm^{-2} at 60 °C, respectively. As suggested by Mukerjee and coworkers [22], the presence of Fe in the binary Pt–Fe catalysts shifts the Pt-oxide formation towards higher potentials, favoring the ORR reaction; but it appears that there is no effect on the ORR rate determining step.

The smaller particle size of the present Pt–Fe catalyst with respect to the Pt catalyst used for comparison could also be responsible of the enhanced activity. Recently, Leger and coworkers [23] have shown enhanced methanol tolerance for ORR of Pt-based catalysts as a function of particle size decrease. Yet, such an effect is not observed for Pt–Cu/C catalyst, which shows a similar activity to Pt/C despite of its particle size is quite small compared to carbon supported pure Pt catalyst (2.1 nm vs 2.8 nm). Furthermore, partial dissolution of iron into the electrolyte from poorly alloyed Pt–Fe catalysts may cause a slight increase in roughness and thus in the number of sites available for the reaction. This aspect was investigated by EDX analysis of the Pt–Fe catalyst before and after operation in acidic solution (Figure 10). This analysis confirms a decrease of Fe content in the catalyst of about 36% with respect to its initial concentration after polarization and cyclic voltammetry experiments in the sulfuric acid solution. This may cause an increase in roughness and surface area.

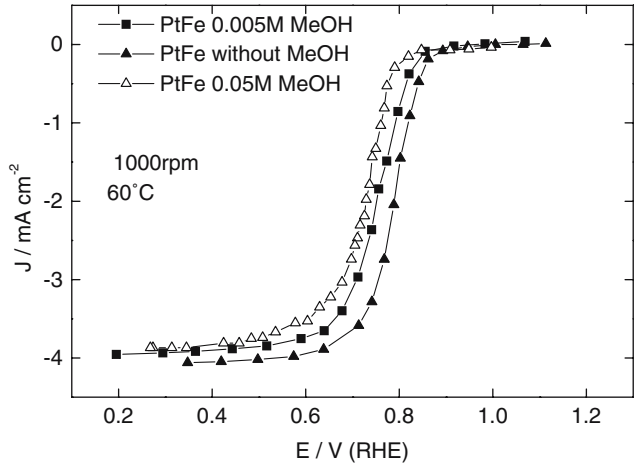

Fig. 6 Polarization curves for ORR in the presence of MeOH at different concentrations in 0.5 M H_2SO_4 at 60 °C, on Pt–Fe/C cathode catalyst.

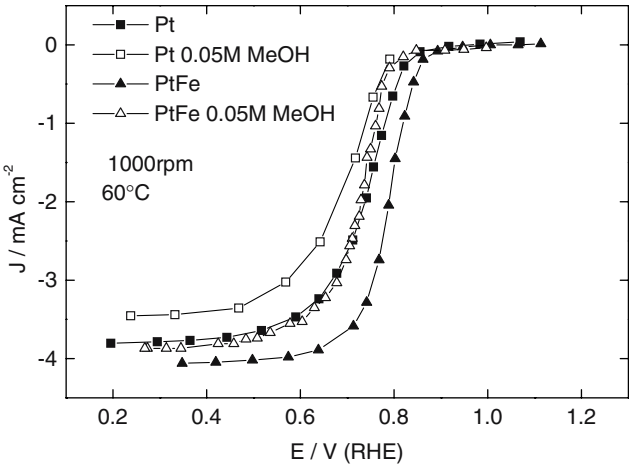

Fig. 7. Polarization curves for ORR at 1000 rpm and 60 °C on different catalysts in 0.5 M H_2SO_4, with and without methanol.

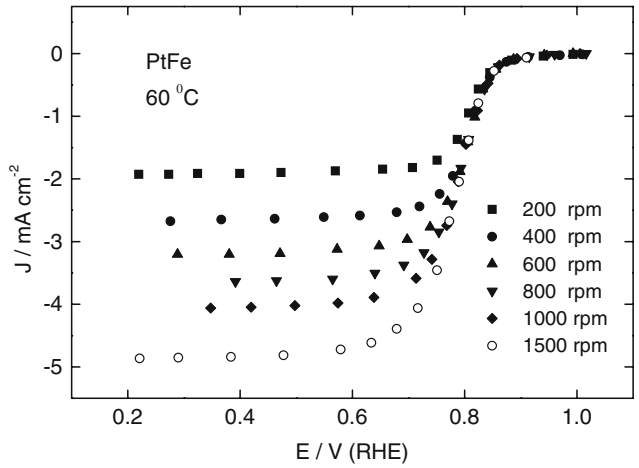

Fig. 8. Polarization curves for ORR at 60 °C and different rotation speeds on the Pt–Fe catalyst in 0.5 M H_2SO_4 in pure oxygen.

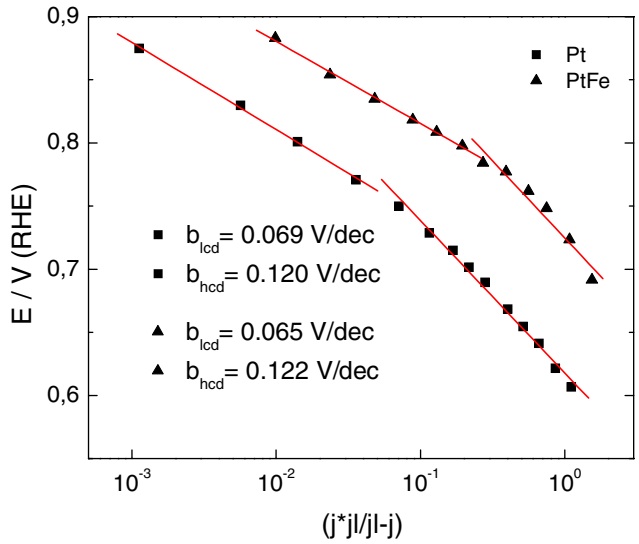

Fig. 9 Tafel plots for ORR in 0.5 M H_2SO_4 on different catalysts.

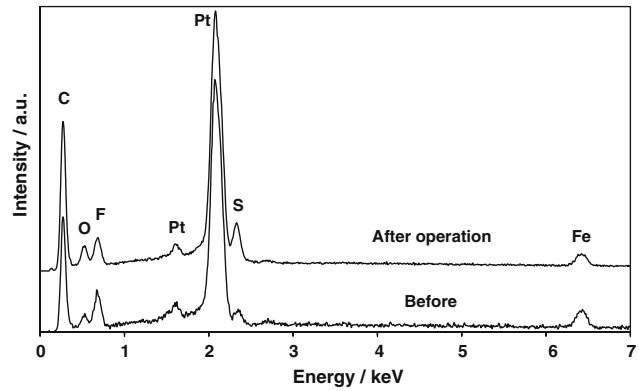

Fig. 10. EDX analysis of the Pt–Fe catalyst before and after operation.

4. Conclusions

A 60 wt% Pt–Fe/C and a 60 wt% Pt–Cu/C catalysts with atomic composition of about Pt_3M_1 were prepared using a colloidal preparation procedure developed at the ITAE Institute that has allowed synthesis of bimetallic catalysts with particle size less than 3 nm and with a suitable degree of alloying. The electrocatalytic behaviour for ORR of these catalysts was investigated by employing the rotating disk technique and compared to that of a pure Pt/C catalyst with similar particle size. No improvement in performance was recorded with the Pt–Cu compared to Pt catalyst, whereas, a promoting effect in enhancing the ORR was observed for the Pt–Fe alloy both with and without methanol in the oxygen-saturated electrolyte solution.

Acknowledgements

The authors gratefully acknowledge support from the MAE-SeCyT Cooperation program; A.M.C.L acknowledges support from CIC de la Provincia de Buenos Aires; CNR-ITAE authors acknowledge support from "Regione Piemonte" through the Micro Cell project (Delibera della Giunta Regionale no 25-14654 del 31/01/05).

References

1. A.S. Aricò, S. Srinivasan and V. Antonucci, *Fuel Cells* **1** (2001) 133.
2. X. Ren, M.S. Wilson and S. Gottesfeld, *J. Electrochem. Soc* **143** (1996) L12.
3. M. Neergat, D. Leveratto and U. Stimming, *Fuel Cells* **2** (2002) 25.
4. S. Wasmus and A. Kuver, *J. Electroanal. Chem.* **461** (1999) 14.
5. A.K. Shukla and R.K. Raman, *Annual Review of Materials Research* **33** (2004) 155.
6. U.A. Paulus, A. Wokaun, G.G. Scherer, T.J. Schmidt, V. Stamenkovic, V. Radmilovic, N.M. Markovic and P.N. Ross, *J. Phys. Chem. B* **106** (2002) 4181.
7. R.C. Koffi, C. Coutanceau, E. Garnier, J.-M. Leger and C. Lamy, *Electrochim. Acta* **50** (2005) 4117.
8. L. Xiong and A. Manthiram, *J. Electrochem. Soc.* **152** (2005) A697.
9. H. Uchida, H. Ozuka and M. Watanabe, *Electrochim. Acta* **47** (2002) 3629.
10. T. Toda, H. Igarashi and M. Watanabe, *J. Electroanal. Chem.* **460** (1999) 258.
11. A.K. Shukla, R.K. Raman, N.A. Choudhury, K.R. Priolkar, P.R. Sarode, S. Emura and R. Kumashiro, *J. Electroanal. Chem.* **563** (2004) 181.
12. C.F. Zinola, A.M. Castro Luna, W.E. Triaca and A.J. Arvia, *J. Applied. Electrochem.* **24** (1994) 119.
13. T. Toda, H. Igarashi, M. Uchida and M. Watanabe, *J. Electrochem. Soc.* **146** (1999) 3750.
14. M. Pourbaix, *Atlas of Electrochemical Equilibria in Aqueous Solutions* (Pergamon, New York, 1966).
15. P.A. Siminov and V.A. Likholobov, Physicochemical aspects of preparation of carbon-supported noble metal catalysts, in A. Wieckowski, E.R. Savinova and C.G. Vayenas (eds) 'Catalysis and Electrocatalysis at Nanoparticle Surfaces', (M. Dekker Inc., 2003), pp. 409–454.
16. M. Watanabe, M. Uchida and S. Motoo, *J. Electroanal. Chem.* **229** (1987) 395.
17. Petrow H.G., Allen R.G. (1976) U.S. Pattern 3,992,331.
18. K. Kinoshita, *J. Electrochem. Soc.* **137** (1990) 845.

19. A.S. Arico, V. Baglio, A. Di Blasi, E. Modica, P.L. Antonucci and V. Antonucci, *J. Electroanal. Chem.* **557** (2003) 167.
20. U.A. Paulus, T.J. Schmidt, H.A. Gasteiger and R.H. Behm, *J. Electroanal. Chem.* **495** (2001) 134.
21. H. Yang, C. Coutanceau, J.-M. Leger, N. Alonso-Vante and C. Lamy, *J. Electroanal. Chem.* **576** (2005) 305.
22. V. Murthi, R.C. Urian and S. Mukerjee, *J. Phys. Chem. B* **108** (2004) 11011.
23. F. Maillard, M. Martin, F. Gloaguen and J.-M. Leger, *Electrochim. Acta* **47** (2002) 3431.